

## SEDIMENTARY ZEOLITES IN THE SIERRA MADRE DEL SUR AND SIERRA MADRE OCCIDENTAL, MEXICO

*Liberto de Pablo-Galán<sup>1</sup>,  
María de Lourdes Chávez-García<sup>2</sup>, and  
Misael Cruz-Sánchez<sup>1</sup>*

### ABSTRACT

Large accumulations of sedimentary zeolites occur in Mexico in the geologic provinces of the Sierra Madre del Sur and the Sierra Madre Occidental. The deposits range from Oligocene to Miocene age. The deposits known in the Sierra Madre del Sur, in the vicinity of Oaxaca, and in the Sierra Madre Occidental, near Guanajuato and San Miguel de Allende, close to the boundary with the Cinturón Volcánico Mexicano, are characterized by the same zeolite minerals, which are clinoptilolite, heulandite, and mordenite. The deposits formed from pyroclastic material of rhyolitic composition deposited in subaerial lacustrine and marine environments. Diagenesis of rhyolitic glass produced: (1) smectite + opal-C; (2) clinoptilolite + opal-C; (3) mordenite + opal-C + K-feldspar; and (4) clinoptilolite + mordenite + opal-C. The formation of zeolites probably involved the removal of SiO<sub>2</sub>, K<sub>2</sub>O, and Na<sub>2</sub>O from the rhyolitic vitric precursor and the enrichment of Al<sub>2</sub>O<sub>3</sub>, MgO, and CaO. Concentrations appear to be limited to SiO<sub>2</sub>/Al<sub>2</sub>O<sub>3</sub> ratios of 4.91-7.14 and (K<sub>2</sub>O+Na<sub>2</sub>O)/(MgO+CaO) ratios of 2.19-0.79.

Key words: Geochemistry, sedimentary zeolites, Sierra Madre del Sur, Sierra Madre Occidental, Mexico.

### RESUMEN

En México hay acumulaciones importantes de zeolitas sedimentarias en las provincias geológicas de la Sierra Madre del Sur y de la Sierra Madre Occidental. Los depósitos son del Oligoceno al Mioceno. Los conocidos en la Sierra Madre del Sur, en las cercanías de Oaxaca, y en la Sierra Madre Occidental, cerca de Guanajuato y San Miguel de Allende, próximos al Cinturón Volcánico Mexicano, contienen los mismos minerales zeolíticos, que son clinoptilolita, heulandita y mordenita. Se formaron de material piroclástico de composición riolítica, depositado en ambientes lacustre y marino. La diagénesis del vidrio riolítico precursor produjo: (1) esmectita + ópalo-C; (2) clinoptilolita + ópalo-C; (3) mordenita + ópalo-C + feldespato potásico, y (4) clinoptilolita + mordenita + ópalo-C. La formación de zeolitas seguramente involucró la separación de SiO<sub>2</sub>, K<sub>2</sub>O y Na<sub>2</sub>O del vidrio riolítico y el enriquecimiento de Al<sub>2</sub>O<sub>3</sub>, MgO y CaO. La cristalización de las zeolitas parece estar limitada a relaciones SiO<sub>2</sub>/Al<sub>2</sub>O<sub>3</sub> de 4.91-7.14 y (K<sub>2</sub>O+Na<sub>2</sub>O)/(MgO+CaO) de 2.19-0.79.

Palabras clave: Geoquímica, zeolitas sedimentarias, Sierra Madre del Sur, Sierra Madre Occidental, México.

### INTRODUCTION

Hydrothermal zeolite minerals are not common in Mexico, usually occurring in minor amounts filling vesicles in extrusive rocks or disseminated in rocks in hydrothermal localities, such as Los Azufres, Michoacán. Secondary zeolites appear to be much more common and widely distributed. Many of such deposits formed during the Oligocene and Miocene, when intensive volcanic activity produced large accumulations of pyroclastics, chiefly in the geological provinces of the Sierra Madre del Sur, the Cinturón Volcánico Mexicano (Mexican Volcanic Belt), and the Sierra Madre Occidental. This paper discusses the geology, mineralogy, geochemistry, and genesis of sedimentary deposits in the Sierra

Madre del Sur and Sierra Madre Occidental, near the cities of Oaxaca and Guanajuato, respectively.

### GEOLOGIC SETTING

The geology of Mexico shows a widespread and abundant distribution of volcanic rocks deposited in lacustrine and marine environments. Prominent volcanic activity during the Oligocene and Miocene developed a huge volcanic plateau in western Mexico, the Sierra Madre Occidental, largely from rhyodacitic and rhyolitic pyroclastic flows (McDowell *et al.*, 1977), marking regression of the Cretaceous and Tertiary inland seas. Large accumulations of glassy pyroclastic rocks were deposited, some of which later altered to zeolites. From the late Miocene onward, a chain of volcanoes formed across Mexico (the Trans-Mexico Volcanic Belt; de Cserna, 1975). In closed basins and fresh lacustrine and marine environments, rhyolitic and rhyodacitic pyroclastics diagenetically altered to zeolites.

<sup>1</sup>Instituto de Geología, Universidad Nacional Autónoma de México, Ciudad Universitaria, Delegación Coyoacán, 04510 D.F., México.

<sup>2</sup>Facultad de Química, Universidad Nacional Autónoma de México, Ciudad Universitaria, Delegación Coyoacán, 04510 D.F., México.

## EXPERIMENTAL WORK

Bulk samples were studied by optical microscopy utilizing thin sections and oil-immersion methods to identify the minerals and their paragenesis. Fine-grained authigenic minerals were identified by X-ray diffraction (XRD), using a Siemens D5000 diffractometer equipped with filtered  $\text{CuK}\alpha$  radiation, scanning at  $1^\circ 2\theta/\text{min}$  over the range  $4^\circ$  to  $60^\circ 2\theta$ . Clay minerals in these samples were solvated by adding ethylene glycol directly to the sample. The relative abundance of minerals was estimated from optical microscopy, XRD, and electron microscopy studies. The abundance of clinoptilolite was determined semiquantitatively from the intensity of  $d_{020} = 8.954 \text{ \AA}$ , using as reference clinoptilolite concentrated from the sampled material with a mixture of bromoform plus acetone. This clinoptilolite concentrate contained minor glass, less than 10%, that could not be loosened by ultrasonic agitation from the intimately associated zeolite. Opal-C was estimated semiquantitatively with reference to  $d_{101} = 4.04 \text{ \AA}$ . To differentiate clinoptilolite from heulandite, samples were heated overnight to  $500^\circ\text{C}$  and analyzed by XRD; those samples that showed no changes other than minor variations in the intensity of the characteristic peaks, were classified as clinoptilolite (Mumpton, 1960; Boles, 1972; Minato *et al.*, 1985). The chemical composition of the tuffs was determined by X-ray fluorescence (XRF) of pressed powders. Na and Mg were measured by flame photometry and wet-chemistry procedures. Loss of ignition was determined at  $850^\circ\text{C}$  on material previously dried at  $60^\circ\text{C}$ ; total Fe is reported as  $\text{Fe}_2\text{O}_3$ . Microtextural relations, morphology, and composition of minerals were determined in flat unpolished specimens by scanning electron microscopy (SEM) coupled with a Kevex energy dispersive spectrometer (EDX) calibrated with glass, feldspar, and kaolinite reference materials. The compositions obtained by this technique, particularly those of selected crystals of diagenetic minerals, are considered semi-quantitative, useful to establish  $\text{SiO}_2/\text{Al}_2\text{O}_3$  and other ratios effective as alternative guides to identification. Infrared absorption spectrometry (IR) was used to identify adsorbed  $\text{H}_2\text{O}$ , oxyhydrils, and certain ionic substitutions, using a Perkin-Elmer 783 double-beam spectrometer, operated at a scanning speed of  $1,000 \text{ cm}^{-1}/\text{min}$  from  $4,000$  to  $2,000 \text{ cm}^{-1}$  and at  $500 \text{ cm}^{-1}/\text{min}$  between  $2,000$  and  $200 \text{ cm}^{-1}$  wavenumbers, on material dried at  $60^\circ\text{C}$  and pressed into KBr discs.

## ZEOLITES IN THE SIERRA MADRE DEL SUR

Zeolitic tuffs occur in the geological province of Sierra Madre del Sur in the State of Oaxaca, southern Mexico (Figure 1). These deposits are exposed along Highway 190, north and south of Oaxaca city, and along the road that connects Salina Cruz on the Pacific coast, with Coatzacoalcos on the eastern coast of the Gulf of Mexico (Mumpton, 1973, 1975; de Pablo-Galán, 1986). The largest outcrops are in the valley of Oaxaca,

in the northwest, in the vicinity of Etna, to the southwest near the town of Tlacolula, and at the eastern and southeastern limits of the city of Oaxaca, between  $16^\circ 50'$  and  $17^\circ 20'$  N and  $96^\circ 10'$  and  $96^\circ 50'$  W (Figure 1).

In total, an extensive area containing zeolite deposits is currently mined for dimensional stone and is of potential interest for other economic applications.

The geology of the area, based on the work of Wilson and Clabaugh (1970), and the geologic map of Oaxaca (Ortega-Gutiérrez *et al.*, 1992), is shown in Figure 1, and the stratigraphic column in Figure 2. The mountainous area surrounding the valley includes Precambrian metasedimentary rocks to the north and west, Cretaceous limestones, sandstone, and shale of the Cuicatlán Formation to the north and southwest, and Tertiary rhyolite, ignimbrite, andesite and basalt flows, and their tuff equivalents, to the east and south. The valley is drained by the Atoyac river, flowing northwest to south. The zeolitic tuffs represent the upper unit of the Miocene Suchilquitongo Formation described by Wilson and Clabaugh (1970), which includes the so-called green-colored Etna Ignimbrite, a tuff consisting of glass shards, pumice, plagioclase phenocrysts, quartz, biotite, and small clay balls deposited in a shallow lacustrine playa (hereafter referred to as the "basin"). Diagenesis of ash-fall material formed the green zeolitic tuffs that now crop out near Etna and in the valley of Oaxaca (Mumpton, 1973, 1975; de Pablo-Galán, 1986).

Vitric tuff overlies Precambrian schist northwest of the basin, northeast of Etna and Magdalena. The upper boundary of the tuff is an essentially unaltered tuff (samples MO8 and MO7; Tables 1 and 2), rhyolitic, containing glass (65 to 90%), pyroclastic sodic plagioclase (3-15%), quartz (3-15%), smectite (3%), minor scoria, tourmaline, hornblende, and oxybiotite (Figures 3 and 4).

The dominant lithology of the area is the zeolitic tuff that crops out in the northwest and in the interior of the basin (Figures 1-4). On the northwestern margin, near Etna, the upper part of the tuff is characterized by phenocrysts of albite (7%) and quartz (5%), pyrogenic grains (3%), rhyolitic bubble-wall glass shards (40%), and authigenic mordenite (30%), opal-C (10%), and K-feldspar (5%) (Table 1). The underlying tuff contains from 20 to 40 wt% glass, and the authigenic mineralogy comprises clinoptilolite (50 to 55%) and opal-C (10%). The lower section of the tuff is characterized by mordenite (20 to 65%), associated with opal-C (5 to 15%) and K-feldspar (5 to 10%), overlying a 2-m-thick bed consisting of clinoptilolite, mordenite, and opal-C; the lower contact is covered. On the southeastern edge of the city of Oaxaca and about the center-point of the basin, glass represents 50% of the tuff and the authigenic minerals are mordenite (25%), opal-C (5-15%), and K-feldspar (5-10%) (Table 1). The composition of the tuff is rhyolitic (Table 2). Glass shards selected from the zeolitic tuff have a rhyolitic composition (Table 3); their refractive index ranges from 1.49 to 1.50. About 5% of the glass shards displays a slightly birefringent outer layer, from which mordenite

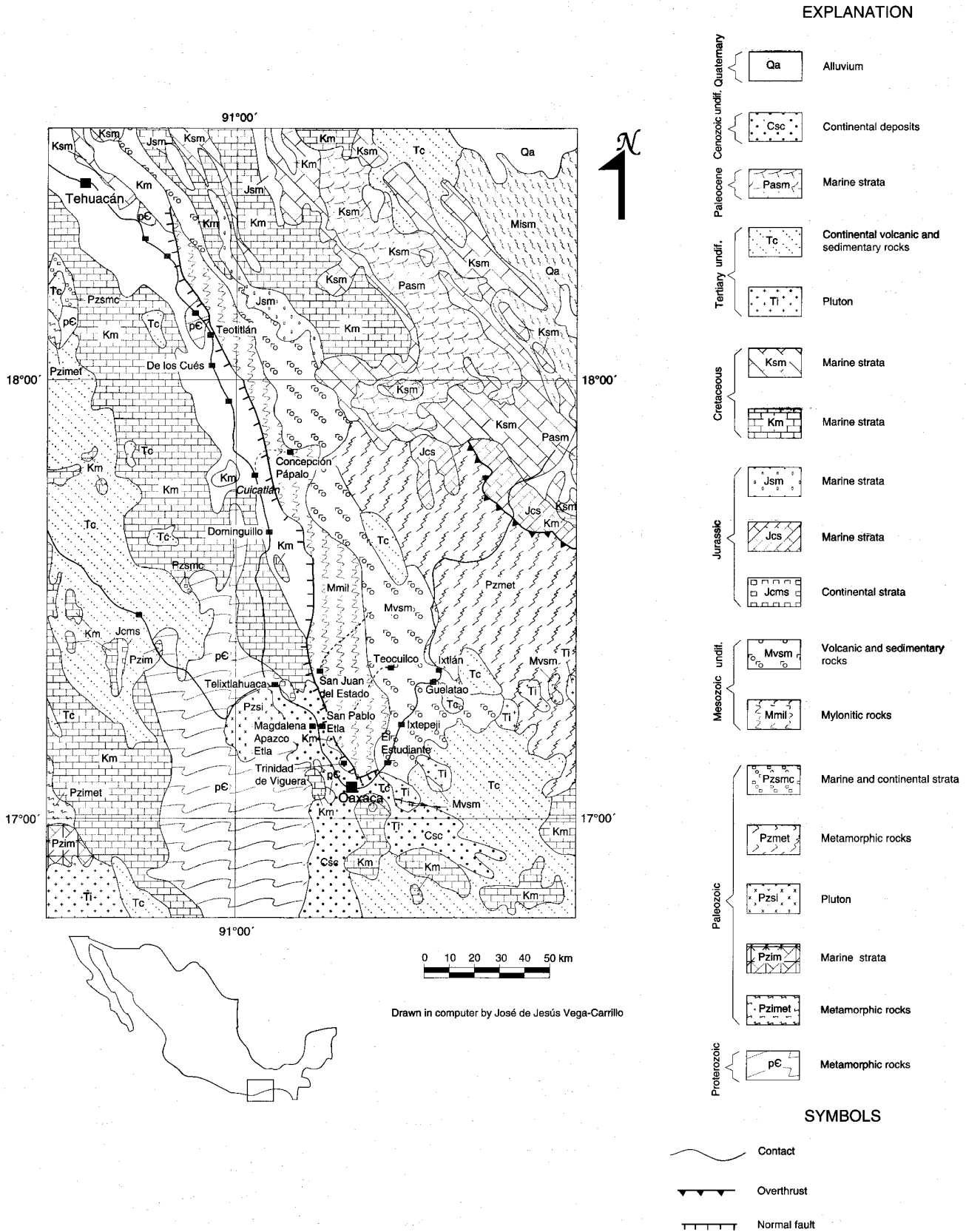


Figure 1. Geologic map of the study area in Oaxaca (Sierra Madre del Sur), with data taken from Wilson and Clabaugh (1970) and Ortega-Gutiérrez and collaborators (1992). The main outcrops of zeolites are located at the northwest and east of the Oaxaca valley and at the southwestern edges of the city of Oaxaca.

Erath.	System	Series	Formation	Column	Lithology
Cenozoic	Quaternary	Holocene	Alluvium		Soil, alluvial deposits
		Pleistocene			
	Tertiary	Pliocene	Etlá, Suchilquitongo		Zeolitic tuff
		Miocene			
		Oligocene			
		Eocene			
Paleocene					

Figure 2. Stratigraphic column of the study area in the Sierra Madre del Sur (data taken from de Cserna, 1965; Ortega-Gutiérrez, 1975; and López-Ramos, 1974).

crystallizes (Figure 5). It has a composition similar to that of the glass, but more hydrated (Table 3).

Mordenite occurs as fibers filling pores (Figure 6). It is the distinctive zeolite in the upper and lower sections of the tuff at Etlá, on the northwestern margins of the depositional basin, and at the southeastern edge of the city of Oaxaca (Figure 4).

Its composition (Table 3), calculated for a 96-oxygen cell (Meier, 1961; Breck, 1974), corresponds to:  $(\text{SiO}_2)_{40}(\text{AlFe}_{0.02}\text{O}_2)_8(\text{Na}_{0.18}\text{K}_{0.23}\text{Ca}_{0.16})_8\text{H}_2\text{O}$ .

From SEM studies, the delicate microtexture of the mordenite crystals suggests that they could have crystallized from solutions (Figure 6, a-d).

Clinoptilolite occurs as well-developed plates crystallized in vesicles or "replacing" glass (Figure 7). This clinoptilolite is stable until 500°C, with only minor reduction of the XRD reflection intensities and broadening of the main peaks (Mumpton, 1960; Breck, 1974; Minato *et al.*, 1985). Its composition (Table 3), calculated for a 72-oxygen cell (Ames, 1960; Alberti, 1975), is represented by the formula  $(\text{Si}_{0.97}\text{Al}_{0.03}\text{O}_2)_{30}(\text{Al}_{1.01}\text{Fe}_{0.12}\text{O}_2)_6(\text{Na}_{0.13}\text{K}_{0.18}\text{Ca}_{0.18}\text{Mg}_{0.03})_6\text{H}_2\text{O}$ .

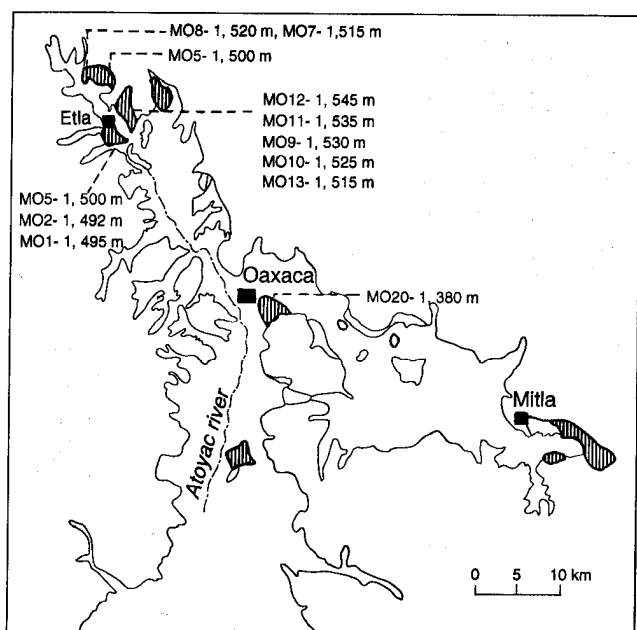


Figure 3. Location map of samples from the study area in Oaxaca. Vertically ruled areas represent outcrops of zeolitic tuffs.

Table 1. Mineralogy of tuffs of the Suchilquitongo Formation, Oaxaca.

Sample	Altitude [m]	Lithology	Cp	Mo	Sm	Op	Kf	Pl	Q	Py	Gl
MO8	1,620	vitric tuff			3			15	15	2	65
MO7	1,615	vitric tuff			3			3	3	1	90
MO12	1,545	zeolitic tuff		30		10	5	7	5	33	40
MO11	1,535	zeolitic tuff	50			10		7	5	3	25
MO9	1,530	zeolitic tuff	50			10		7	5	3	25
MO10	1,525	zeolitic tuff	55			10		7	5	3	20
MO13	1,515	zeolitic tuff	50			10		7	5	3	25
MO5	1,500	zeolitic tuff		65		tr		7	5	3	20
MO1	1,495	zeolitic tuff		25		15		7	5	3	40
MO3	1,490	zeolitic tuff		20		5		7	5	3	50
MO2	1,482	zeolitic tuff		25		15		7	5	3	20
MO20	1,380	zeolitic tuff		25		5		7	5	3	50

It is the predominant zeolite in the middle section of the tuff (Figure 4). SEM studies show clinoptilolite "replacing" glass bubbles (Figure 7, a), as parallel well-packed crystals that could have crystallized from leached rhyolitic glass (Figure 7, b), or well-formed, in vugs, where they formed from solutions (Figure 7, c). Intermixed with clinoptilolite are thick tabular and blocky crystals of possible heulandite or Ca-rich clinoptilolite, of composition more calcic than clinoptilolite (Figure 8). It is in low concentration, insufficient to identify it positively by XRD as per its characteristic transformation at 300°C (Mumpton, 1960; Breck, 1974; Minato *et al.*, 1985).

It has a composition (Table 3) that, calculated to a 72-oxygen cell (Merkle and Slaughter, 1968), corresponds to

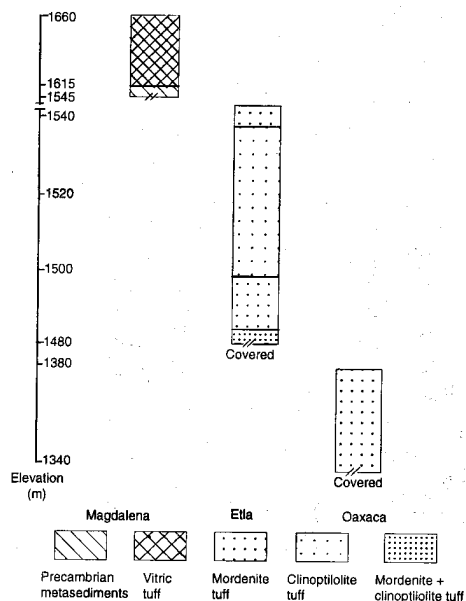


Figure 4. Schematic columnar sections of Oaxaca (Sierra Madre del Sur). The vitric tuffs overlie the Precambrian metasediments to the northwest of the area in the vicinity of Magdalena and Etlá. The zeolitic tuffs have their lower contacts covered by alluvium.

Table 2. Chemical composition of tuffs of the Suchilquitongo Formation, Oaxaca.

Sample*	MO8	MO7	MO12	MO11	MO9	MO10	MO13	MO5	MO1	MO3	MO2	MO20
Altitude (m)	1,620	1,615	1,545	1,535	1,530	1,525	1,515	1,500	1,495	1,490	14,82	1,380
Lithology	Vitric	Vitric	Zeolitic	Zeolitic	Zeolitic	Zeolitic	Zeolitic	Zeolitic	Zeolitic	Zeolitic	Zeolitic	Zeolitic
SiO <sub>2</sub> (wt. %)	67.91	66.51	68.80	68.16	66.49	67.67	67.56	66.28	67.45	67.40	66.21	67.49
Al <sub>2</sub> O <sub>3</sub>	14.87	13.38	13.47	14.25	13.47	14.08	13.65	13.46	14.49	14.29	14.20	14.14
Fe <sub>2</sub> O <sub>3</sub>	1.49	2.05	1.56	1.50	1.48	1.57	1.72	2.33	1.54	1.29	1.99	1.65
MgO	1.12	1.78	0.91	1.05	1.72	1.21	1.36	1.23	0.90	1.24	0.90	1.15
CaO	1.25	1.75	1.25	1.50	2.31	1.72	1.93	1.86	1.23	1.72	1.65	1.56
Na <sub>2</sub> O	3.45	2.25	3.60	3.68	3.01	3.28	3.02	2.79	3.75	2.85	3.21	3.25
K <sub>2</sub> O	3.41	3.02	3.10	3.52	2.22	2.90	2.74	2.60	2.86	3.28	4.35	3.46
H <sub>2</sub> O <sup>+</sup>	2.48	5.19	5.63	4.97	7.13	6.03	6.45	6.30	5.76	6.01	5.46	5.61
H <sub>2</sub> O <sup>-</sup>	3.71	3.86	1.10	1.36	2.16	1.46	1.52	2.93	2.02	1.91	2.01	1.41
Total	99.69	99.79	99.42	100.00	99.99	99.92	99.95	99.78	100.00	99.99	99.98	99.72

$(\text{Si}_{0.94}\text{Al}_{0.06}\text{O}_2)_{30}(\text{Al}_{0.90}\text{Fe}_{0.02}\text{O}_2)_6(\text{Na}_{0.33}\text{K}_{0.20}\text{Ca}_{0.45}\text{Mg}_{0.02})_6 \cdot \text{H}_2\text{O}$ . Opal-C spheres are seen in the SEM studies as well-

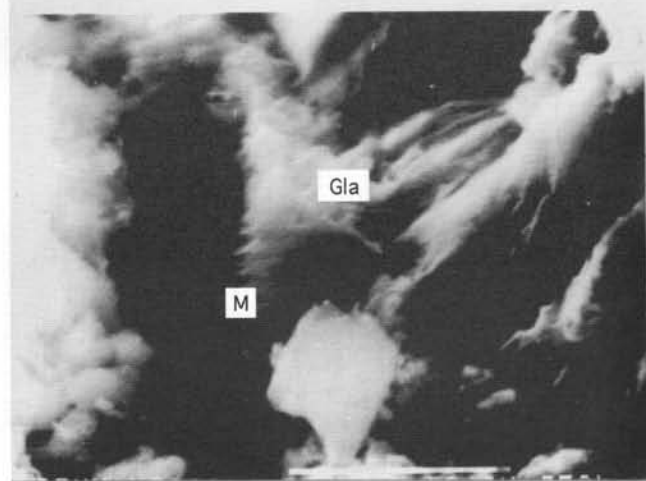
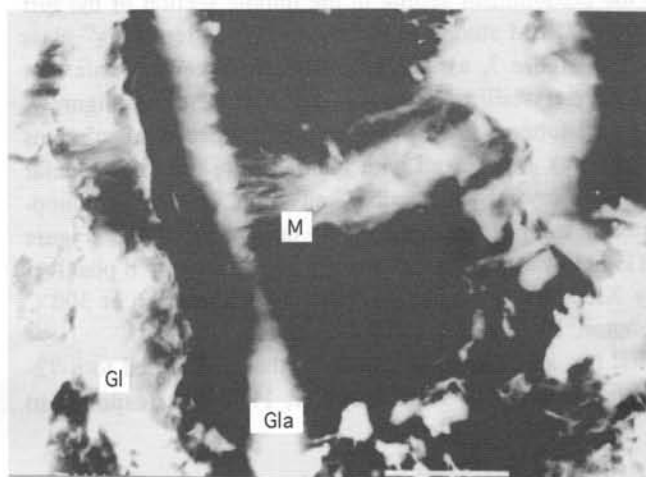


Figure 5. SEM photomicrographs showing glass and glass altering to mordenite, sample MO20. Gl: glass, Gla: altered glass, M: mordenite, Op: opal-C. Horizontal bar represents 1  $\mu\text{m}$ .

formed aggregates of crystallites (Figures 6-8). It is characterized by the 4.05Å cristobalite reflection in XRD patterns. K-feldspar occurs in the mordenite-rich tuffs, but it was not detected in the clinoptilolite-rich tuffs.

Two facies are recognized in Oaxaca. One is fresh vitric rhyolitic tuff that is unconsolidated, medium-grained, and contains colorless subangular shards, minor pumice, scoria, sodic

Table 3. Average chemical composition (wt%) of rhyolitic glass, altered glass, mordenite, clinoptilolite and heulandite from tuffs of the Suchilquitongo Formation, Oaxaca.

	Rhyolitic glass	Altered glass	Mordenite	Clinoptilolite	Heulandite
SiO <sub>2</sub> (wt%)	69.00	68.10	70.00	68.90	63.30
Al <sub>2</sub> O <sub>3</sub>	14.80	10.50	11.80	14.10	13.70
Fe <sub>2</sub> O <sub>3</sub>	1.52	0.91	0.46	2.30	na
MgO	0.13	0.39	na	0.29	0.21
CaO	2.46	3.38	2.14	2.34	5.58
Na <sub>2</sub> O	1.59	1.03	1.33	0.99	2.31
K <sub>2</sub> O	2.55	1.55	2.53	2.09	2.10
Total	91.96	85.86	87.94	91.03	87.18
Si			40.00	29.08	28.37
Al			8.00	6.99	7.22
Fe			0.20	0.73	na
Mg			na	0.18	0.14
Ca			1.31	1.06	2.68
Na			1.41	0.81	2.00
K			1.87	1.11	1.20
O			96	72	72
Si/Al			4.64	4.16	3.94
Si/(Al+Fe)			4.54	3.77	3.94
Na+K+Ca+Mg			3.31	3.16	6.02
Si+Al+Fe			36.57	36.80	35.59

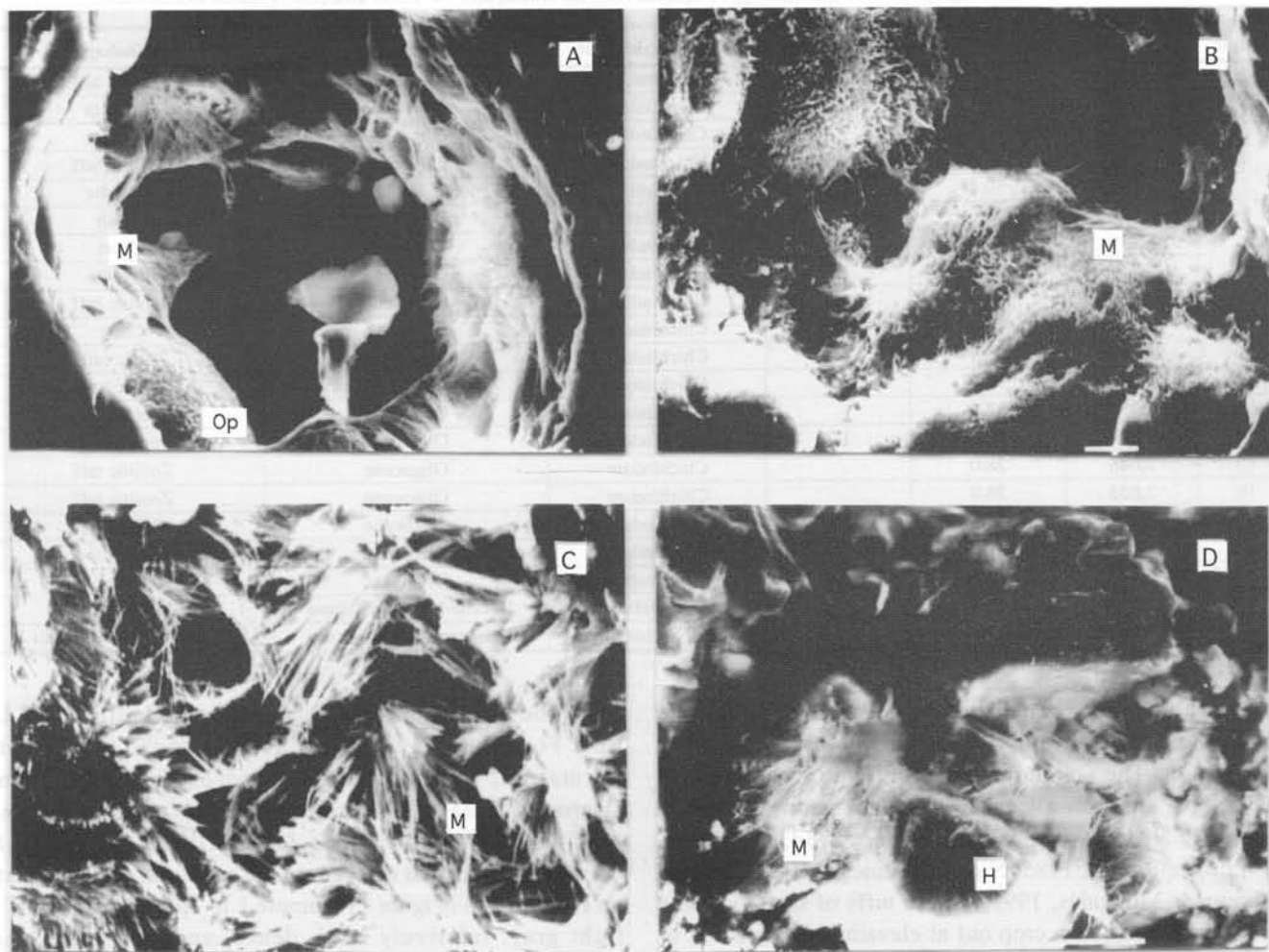


Figure 6. SEM photomicrographs of mordenite: (A, B, C) crystallized in vesicles; (D) covering blocky clinoptilolite. M: mordenite, Cl: clinoptilolite, H: heulandite or Ca-rich clinoptilolite, Op: opal-C, Gl: glass. Samples MO12 and MO2, Etlá, Oax. Horizontal bar represents 1  $\mu\text{m}$ .

plagioclase, quartz, biotite, and smectite. It crops out as the upper tuff, overlying the zeolitic tuff at Magdalena, at elevations from 1,615 to 1,660 m (Figure 4). Two distinct lithologic units can be recognized in this facies; a lower bed containing about 90% glass, 3% subangular sodic plagioclase, 3% quartz, 3% smectite, and 1% of tourmaline, hornblende, oxybiotite, pumice, and scoria (sample MO7 in Tables 1 and 2); and an upper bed, which is more crystalline and contains rhyolitic glass (65%), subangular albite (15%), quartz (15%), pyrogenic grains (2%), and smectite (3%) (sample MO8 in Tables 1 and 2). The glass has a refraction index of 1.50, which corresponds to a rhyolitic composition. Chemical data indicate that within this essentially fresh vitric tuff, the contents of Si, Al, Na, and K decrease with elevation, whereas the contents of Ca, Mg, and  $\text{H}_2\text{O}$ , and the ratio Si/Al increase. A second diagenetic facies corresponds to zeolitic tuff that is green, medium to fine grained, poor to moderately well-sorted, porous, silicified, and relatively hard. This facies is characterized by two distinct authigenic assemblages: one consisting of mordenite + opal-C + K-feldspar, and the other of clinoptilolite + opal-C. The microtexture

observed by SEM suggests that this mordenite could have crystallized from solutions, whereas clinoptilolite could have replaced the leached glass or crystallized from solutions.

#### ZEOLITES IN THE SIERRA MADRE OCCIDENTAL

Sedimentary zeolites occur southeast of the geological province of the Sierra Madre Occidental, close to the boundary with the Mexican Volcanic Belt (Figure 9). The zeolitic tuff is well exposed along highway 45, between the cities of Juventino Rosas and Guanajuato, between  $20^{\circ}52'$  and  $21^{\circ}00'$  N and  $101^{\circ}00'$  and  $101^{\circ}19'$  W. The area is characterized by alluvial plains, hills, mesas, and basins filled with volcanic rocks. To the west and northwest of the zeolitic deposits, continental clastic rocks of the Paleocene and Eocene Red Conglomerate crop out and are overlain by tuffaceous sandstone of the Eocene Losero Formation (Figures 9 and 10).

Welded tuff of rhyolitic composition of the late Eocene and Oligocene La Bufa Formation underlies rhyolite flows, vitric and zeolitic tuffs of the Oligocene Chichindaro Formation, which are overlain by andesitic to trachyandesitic

Table 4. Localities, stratigraphic units, and lithology of samples from the Guanajuato—J. Rosas area (Sierra Madre Occidental).

Sample	Altitude [m]	Location [km]*	Length [km]*	Stratigraphic unit	Period	Lithology
1	1,772	60.7	25.7	La Bufa	Eocene-lower Oligocene	Welded tuff
2	1,860	59.1	1.6	Chichíndaro	Oligocene	Rhyolite
3	1,938	57.8	7.3	Chichíndaro	Oligocene	Rhyolite
4	1,962	51.8	0	Chichíndaro	Oligocene	Zeolitic tuff
5	2,035	50.4	0.9	Cedros	Oligocene-lower Miocene	Andesite
6	2,120	48.7	1.7	Cedros	Oligocene	Basalt
7	2,170	43.5	4.8	Chichíndaro	Oligocene	Chert
8	2,174	42.3	1.6	Chichíndaro	Oligocene	Rhyolite
9	2,182	42.3		Chichíndaro	Oligocene	Zeolitic tuff
10	2,170	40.0	2.0	Chichíndaro	Oligocene	Chert
11	2,090	35.5	3.8	Chichíndaro	Oligocene	Vitric tuff
12	1,995	32.9	2.6	Chichíndaro	Oligocene	Vitric tuff
13	1,995	32.9		Chichíndaro	Oligocene	Zeolitic tuff
14	2,010	29.3	1.7	Chichíndaro	Oligocene	Zeolitic tuff
15	2,046	28.0		Chichíndaro	Oligocene	Zeolitic tuff
16	2,055	28.0		Chichíndaro	Oligocene	Zeolitic tuff
17	2,035	28.0	5.7	Chichíndaro	Oligocene	Zeolitic tuff
20	2,040	21.2	1.5	Chichíndaro	Oligocene	Rhyolite
	2,030	19.7	1.6	Chichíndaro	Oligocene	Chert
21	1,920	16.6	4.1	La Bufa	Eocene-lower Oligocene	Welded tuff
	1,850	12.5	12.3	Red Conglomerate	Paleocene-lower Eocene	Continental clastics

lavas of the Cedros Formation. Late Miocene and Pliocene volcanism is represented by lava flows and tuffs of rhyolitic composition. The Quaternary section is characterized by basaltic lava and scoria located in the southern part of this area (CETENAL, 1973a, 1973b, 1973c, 1973d; de Cserna, 1975; López-Ramos, 1985; Nieto-Samaniego, 1992; Consejo de Recursos Minerales, 1992). These tuffs of the Oligocene Chichíndaro Formation crop out at elevations from 1,962 to 2,055 m and between 2,174 and 2,182 m (de Pablo-Galán *et al.*, 1994; de Pablo-Galán and Chávez-García, 1996).

The dominant lithologies are welded tuff of the La Bufa Formation, rhyolite and its tuffs of the Chichíndaro Formation, andesite of the Cedros Formation, and Quaternary basalt (Figures 10 and 11). Welded tuff, representing the upper Eocene-lower Oligocene La Bufa Formation, crops out 60.7 km to the southeast of Guanajuato on Highway 45 (Figure 11; sample 1 in Table 4). This tuff is light gray, relatively hard, dense, and coarse-grained. Pyrogenic crystals include quartz (10 wt%), sanidine (5%), traces of biotite and magnetite and occur in a partially devit-

Table 5. Mineralogy of rocks of the La Bufa and Chichíndaro Formations.

Sample	Stratigraphic unit	Lithology	Cp	Mo	Sm	Op	Q	Kf	Sa	Pl	Bi	Gl
1	La Bufa	Welded tuff				30	10	20	5		tr	35
2	La Bufa	Rhyolite			5	5	40		40	5	5	
3	La Bufa	Rhyolite			5	5	40		40	10	tr	
4	La Bufa	Zeolitic tuff	60			5	5				tr	30
5	Cedros	Andesite										
7	Quaternary	Basalt										
8	Quaternary	Chert										
9	Chichíndaro	Rhyolite			5		40		45	10		
10	Chichíndaro	Zeolitic tuff	75			5						20
11	Chichíndaro	Vitric tuff			30	10	5	10		5		40
12	Chichíndaro	Vitric tuff	10		25	30	5	5	tr			20
13	Chichíndaro	Zeolitic tuff	45			20	5		5	5		20
14	Chichíndaro	Zeolitic tuff	50	tr		10	5		5			30
15	Chichíndaro	Zeolitic tuff	65			20			5			10
16	Chichíndaro	Zeolitic tuff	65			10					tr	25
17	Chichíndaro	Zeolitic tuff	60			10	5		5	5	5	10

Mineralogy determined by X-ray diffraction and optical microscopy. Numbers represent estimated mineral abundance in weight percent. Cp, clinoptilolite; Mo, mordenite; Sm, smectite; Op, opal-C; Q, quartz; Kf, K-feldspar; Sa, sanidine; Pl, plagioclase; Bi, biotite; Gl, glass.

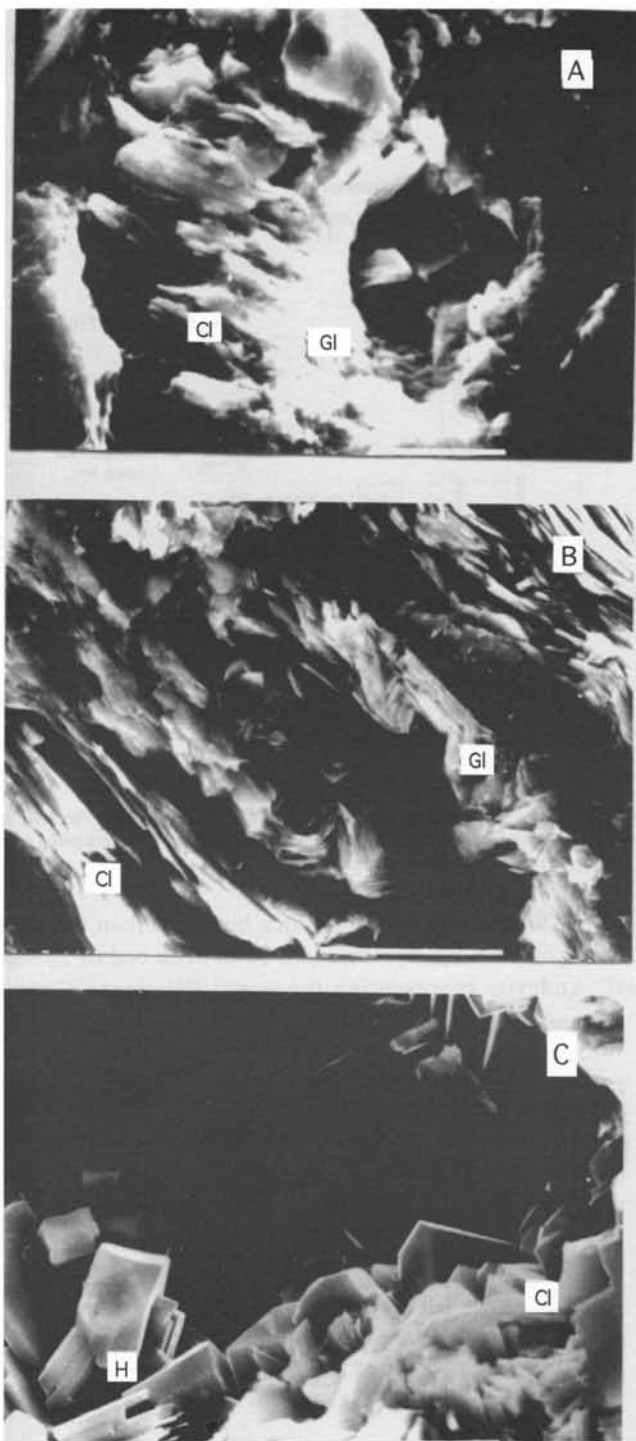


Figure 7. SEM photomicrographs showing clinoptilolite: (A) replacing glass, sample MO5; (B) replacing glass, sample MO13; (C) crystallized in vesicles, sample MO10. Cl: clinoptilolite, H: heulandite, Op: opal-C, Gl: glass. Etna, Oax. Horizontal bar represents 10  $\mu\text{m}$ .

rified vitreous matrix. Bubble-wall glass shards represent 35% of the rock and are partly devitrified to K-feldspar + opal-C (Table 5). The composition is rhyolitic (Table 6). The ratios  $\text{SiO}_2/\text{Al}_2\text{O}_3$  and  $(\text{Na}_2\text{O}+\text{K}_2\text{O})/(\text{MgO} + \text{CaO})$  are about the same as those of the overlying rhyolite and much higher

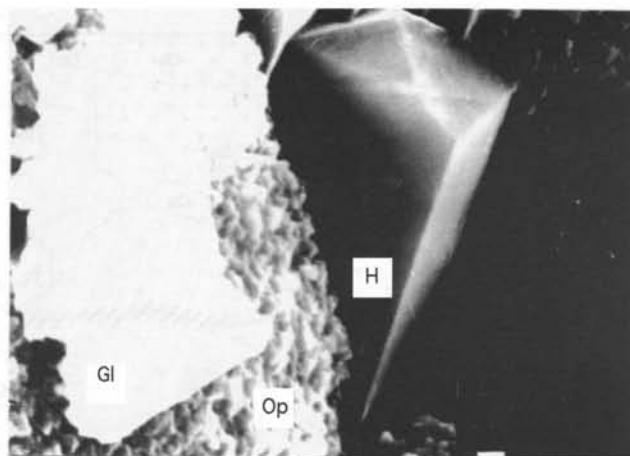
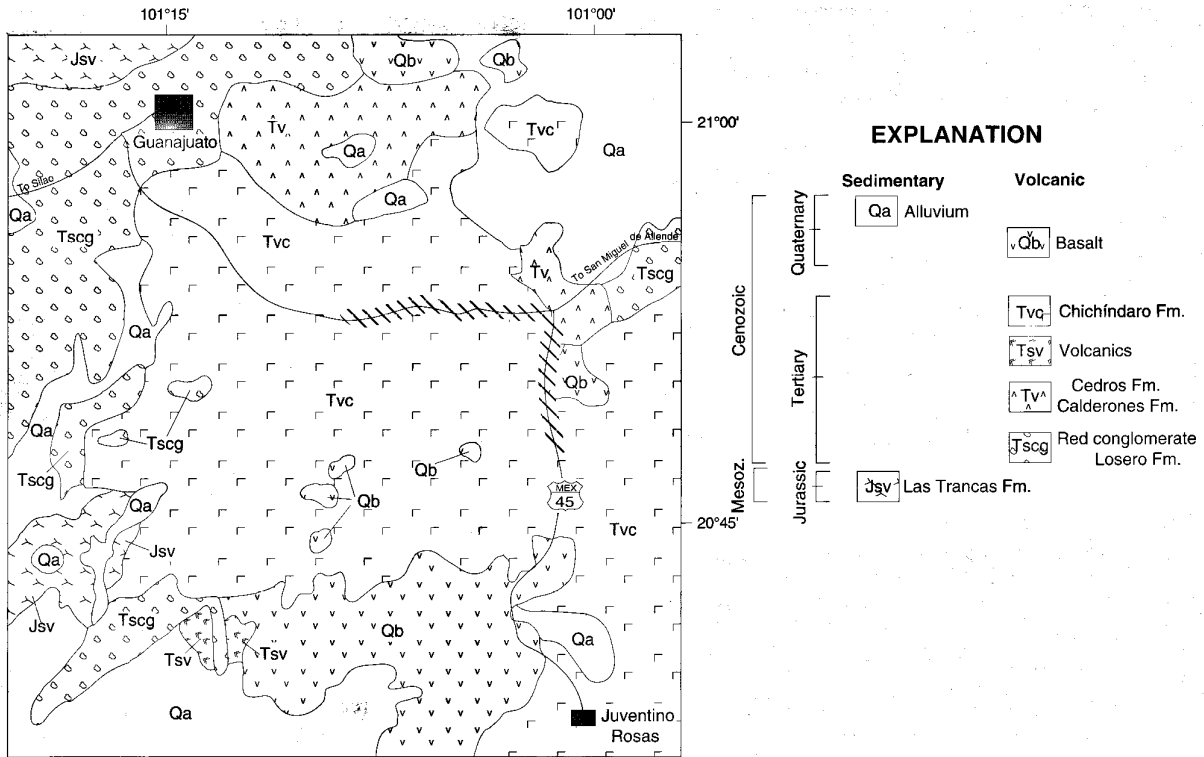


Figure 8. SEM photomicrograph of Ca-rich or heulandite associated with opal-C and glass. H: heulandite or Ca-rich clinoptilolite, Gl: glass, Op: opal-C. Sample MO5, Etna, Oax. Horizontal bar represents 1  $\mu\text{m}$ .

than those corresponding to the zeolitic and vitric tuffs in the region (Figure 12).

The overlying Oligocene Chichindaro Formation can be differentiated into three subunits. Sub-unit 1, which is the lowest, is a rhyolite that crops out 59.1 km and 42.3 km southeast Guanajuato along Highway 45 (Figure 9; samples 2, 3, and 9 in Tables 4 and 5). It is brick-red, hard, dense, porphyritic hypidiomorphic, and contains smectite (5%), phenocrysts of quartz (40%), sanidine (40%), and albite (10%), and traces of biotite. The chemical composition corresponds to a potassic rhyolite with  $\text{SiO}_2/\text{Al}_2\text{O}_3$  and  $(\text{Na}_2\text{O}+\text{K}_2\text{O})/(\text{CaO}+\text{MgO})$  ratios similar to those of the underlying welded tuff of the La Bufa Formation (Table 6, Figure 12). Sub-unit 2 overlies sub-unit 1; it is a vitric tuff which crops out from 40.3 to 32.9 km to the southeast of Guanajuato (Figure 9; samples 11 and 12 in Table 4). It is pale brown, coarse, and contains pyrogenic quartz (5%), intermediate plagioclase (5%), and traces of sanidine. Bubble-wall glass shards, representing from 20 to 40% of the rock, are partly altered to authigenic smectite and opal-C. Chemical data indicate that the tuff contains less  $\text{SiO}_2$ ,  $\text{Na}_2\text{O}$ , and  $\text{K}_2\text{O}$  and more  $\text{Al}_2\text{O}_3$ ,  $\text{CaO}$ , and  $\text{MgO}$  than the vitric tuff, and has  $\text{SiO}_2/\text{Al}_2\text{O}_3$  and  $(\text{Na}_2\text{O}+\text{K}_2\text{O})/(\text{CaO}+\text{MgO})$  ratios significantly lower than those typical of the rhyolite (Table 6, Figure 12). Sub-unit 3 corresponds to the middle section of the zeolitic tuff and crops out from 51.8 km to 22.3 km to the southeast of Guanajuato (Figure 9; samples 4, 10, and 13-17 in Tables 4 and 5). It is pale yellowish-green to pink-gray, granular, and light. Pyrogenic quartz, sanidine, plagioclase, and biotite constitute less than 10% of the rock. Bubble-wall glass shards are substantially devitrified to zeolite, leaving about 10-20% unaltered glass. The principal authigenic mineral is clinoptilolite, which represents from 45 to 75 wt% of the rock and coexists with opal-C (5-20%). Mordenite occurs at relatively higher elevations, in a silicic, low- $\text{Al}_2\text{O}_3$  bed (Figure 9; Table 5). Above 2,055 m, the tuff contains lapilli of rhyolite.





Computer drawing by José de Jesús Vega Carrillo

Figure 9. Geologic map showing the area of zeolitic tuffs in the Sierra Madre Occidental close to the boundary with the Mexican Volcanic Belt, in the State of Guanajuato. The tuffs crop out along Highway 45 from Guanajuato to Juventino Rosas. Samples were collected along the cross-hatched area. With data taken after CETENAL (1973a, 1973b, 1973c, 1973d) and Consejo de Recursos Minerales (1992). After de Pablo-Galán and Chávez-García (1996).

The  $SiO_2/Al_2O_3$  and  $(Na_2O+K_2O)/(CaO+MgO)$  ratios are 5.98 and 1.35, respectively. The zeolitic tuff shows the diagenetic facies clinoptilolite + opal-C, and clinoptilolite + mordenite +

opal-C. Chert occurs in a 4-m-thick bed, underlain by vitric tuff and overlain by rhyolite and a 10-m-thick bed of zeolitic tuff. Andesite representing the upper Oligocene Cedros

Era	System	Series	Formation	Column	Lithology
Cenozoic	Quaternary	Holocene	Alluvium		Alluvial deposits
		Pleistocene	Basaltic volcanism		Lava flows and scoria of basaltic composition
	Tertiary	Pliocene	Continental deposits		Continental deposits
			Volcanic rocks		Lava flows and tuffs of rhyolitic composition
		Oligocene	Cedros		Lava flows of andesitic composition
			Calderones		Volcanoclastic of intermediate composition
			Chichindaro		Zeolitic tuff, rhyolitic composition Rhyolite flows
		Eocene	La Bufa		Welded tuff, rhyolitic composition
			Losero		Tuffaceous sandstone
		Paleocene	Red conglomerate		Continental clastics
Mesozoic	Jurassic	Upper	Las Trancas		Sedimentary deposits

Figure 10. Stratigraphic column of the southwest portion of the State of Guanajuato, with data after López-Ramos (1985), Nieto-Samaniego (1992), and Consejo de Recursos Minerales (1992).

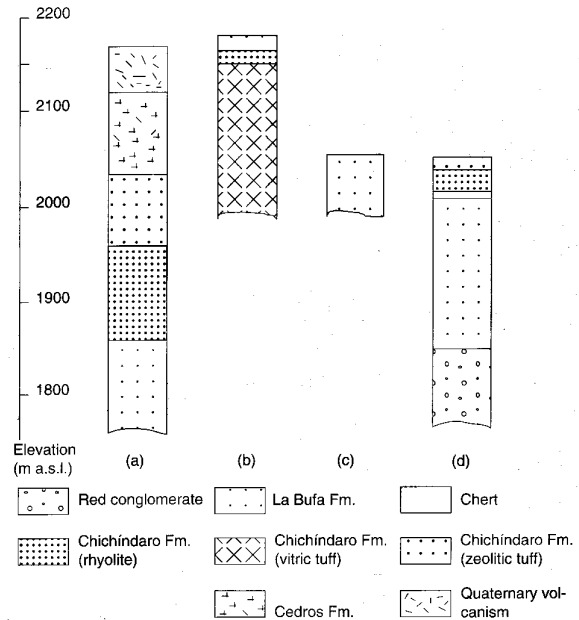


Figure 11. Schematic columnar sections of the Guanajuato-Juventino Rosas area: (a) 50 km southeast Guanajuato; (b) 40 km; (c) 30 km; (d) 22 km (de Pablo-Galán and Chávez-García, 1996).

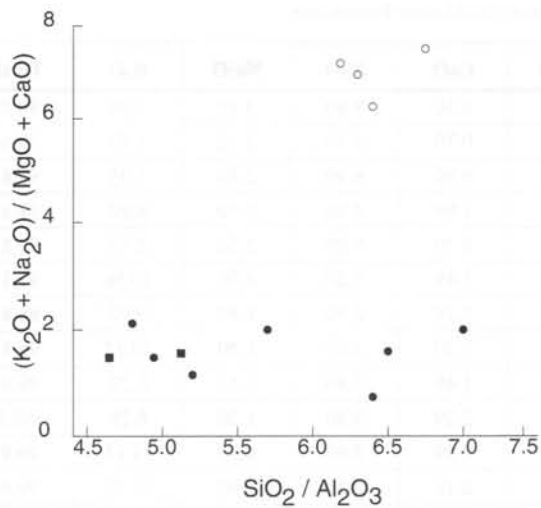
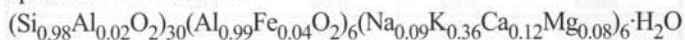


Figure 12. Variation in the ratio  $\text{SiO}_2/\text{Al}_2\text{O}_3$  vs.  $(\text{K}_2\text{O} + \text{Na}_2\text{O})/(\text{MgO} + \text{CaO})$ . The La Bufo ignimbrite and the Chichindaro rhyolite maintain  $\text{SiO}_2/\text{Al}_2\text{O}_3$  ratios between 6.38 and 6.81 whereas the vitric and zeolite tuffs sustain  $(\text{K}_2\text{O} + \text{Na}_2\text{O})/(\text{MgO} + \text{CaO})$  below 2.19. Open circles: ignimbrite and rhyolite; solid circles: zeolitic tuffs; solid boxes: vitric tuff.

Formation is slightly altered to smectite. Quaternary volcanism is characterized by the olivine basalt flows that crop out at 48.7 km to the southeast of Guanajuato.

The authigenic minerals are clinoptilolite, mordenite, opal-C, K-feldspar, smectite, and quartz. Clinoptilolite occurs in well-formed platy and blocky crystals replacing glass or uniformly disseminated in the rock (Figure 13). Clinoptilolite makes up from 45 to 75% by weight of the zeolitic tuff, and coexists with an estimated 10 to 30% glass, 10-20% opal-C, and 8% total of pyroclastic quartz, sanidine, albite, and biotite. Clinoptilolite does not occur in the La Bufo welded tuff. The composition of this clinoptilolite (Table 7), calculated for a 72-oxygen cell (Breck, 1974; Alberti, 1975; Alietti, 1972), corresponds to the formula:



Mordenite occurs as thin less than 1- $\mu\text{m}$ -thick fibers associated with clinoptilolite (sample 14, Table 4). Some fibers resemble pseudomorph bubble-wall glass (Figure 14). The composition calculated for a 96-oxygen cell corresponds to  $(\text{Si}_{0.99}\text{Al}_{0.01}\text{O}_2)_{40}(\text{Al}_{0.97}\text{Fe}_{0.04}\text{O}_2)_8(\text{Na}_{0.10}\text{K}_{0.13}\text{Ca}_{0.19}\text{Mg}_{0.14})_8\cdot\text{H}_2\text{O}$ . The Si/Al ratio is 4.88, higher than the 4.51 value of clinoptilolite. The very fine crystallization observed for mordenite through SEM studies indicates that this mordenite may have precipitated from solution rather than be formed from precursor clinoptilolite. Opal-C spheres, about 10  $\mu\text{m}$  in diameter, are conspicuous in the SEM (Figures 13-15). Dioctahedral smectite occurs in small amounts, about 5 wt%, associated with opal-C in rhyolite and about 25-30% in vitric tuff associated with opal-C or with clinoptilolite + opal-C (sample 12, Table 5). K-feldspar is associated with opal-C in devitrified bubble-wall glass shards in vitric tuffs, different from the pyrogenic sanidine phenocrysts. The K-feldspar was not observed in these zeolitic tuffs. Authigenic quartz occurs in vitric and zeolitic tuffs, char-

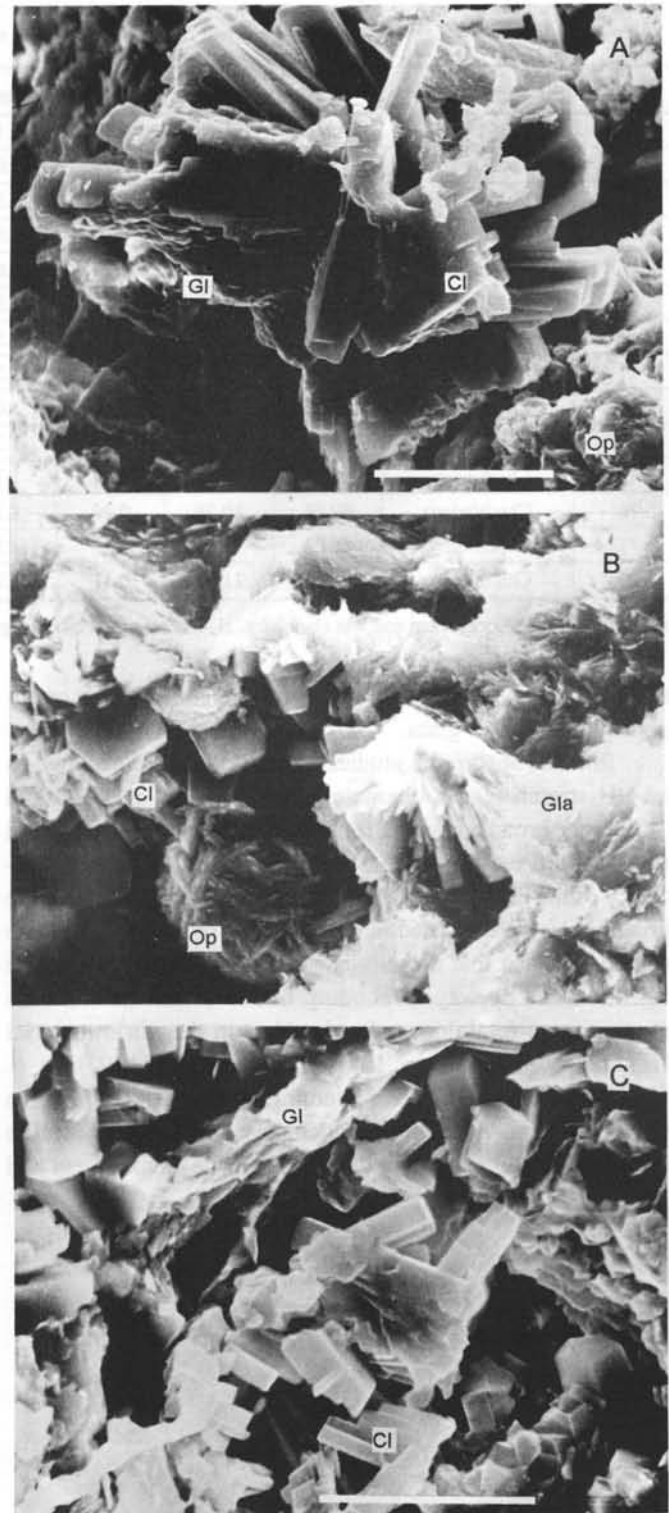


Figure 13. SEM photomicrographs of clinoptilolite: (A) crystallized from bubble-glass; (B) crystallizing from altered glass or from solutions; (C) disseminated in the tuff. Cl: clinoptilolite, Gl: glass, Gla: altered glass, Op: opal-C. Guanajuato. Horizontal bar represents 10  $\mu\text{m}$ .

acterized by its saccaroidal microtexture and undulatory extinction, distinct from pyrogenic quartz. Bubble-wall glass shards occur unaltered, pitted, and replaced by clinoptilolite and mordenite. The concentration of glass ranges from 10 to 40%; its

Table 6. Chemical composition of rocks of the La Bufa and Chichíndaro Formations.

Sample	Stratigraphic unit	SiO <sub>2</sub>	Al <sub>2</sub> O <sub>3</sub>	TiO <sub>2</sub>	Fe <sub>2</sub> O <sub>3</sub>	MgO	CaO	K <sub>2</sub> O	Na <sub>2</sub> O	H <sub>2</sub> O	Total
1	La Bufa	75.46	11.40	0.11	1.10	0.74	0.30	4.60	3.10	2.66	99.8
2	Chichíndaro	75.16	11.89	0.11	1.05	0.61	0.70	5.50	3.10	1.49	99.6
3	Chichíndaro	73.47	11.81	0.11	1.34	0.76	0.50	6.30	2.50	3.05	99.8
4	Chichíndaro	68.70	12.06	0.11	1.34	0.97	1.69	4.10	1.50	8.98	99.4
9	Chichíndaro	74.13	11.61	0.17	1.62	0.45	0.70	5.80	2.50	2.70	99.8
10	Chichíndaro	64.90	13.21	0.15	1.39	1.32	1.49	5.20	0.90	10.56	99.1
11	Chichíndaro	64.75	13.29	0.53	1.36	1.49	2.19	3.50	1.80	9.93	98.8
12	Chichíndaro	68.13	13.06	0.11	1.34	1.11	1.20	2.10	1.50	10.12	98.8
13	Chichíndaro	74.26	11.19	0.10	1.05	1.29	1.49	2.80	1.50	6.22	99.9
14	Chichíndaro	74.15	10.38	0.10	1.34	0.97	2.29	3.30	1.20	6.28	100.0
15	Chichíndaro	66.27	13.11	0.17	1.39	0.99	2.29	3.60	0.90	11.15	99.9
16	Chichíndaro	69.68	10.76	0.20	1.39	1.54	2.19	2.20	0.80	11.14	99.9
17	Chichíndaro	66.88	12.70	0.13	1.34	1.59	2.29	3.40	1.20	10.30	99.8
20	Chichíndaro	74.65	11.81	0.11	1.90	0.27	0.30	4.80	3.40	2.15	99.4

Analysis by X-ray fluorescence and wet chemistry. H<sub>2</sub>O determined by loss ignition at 850° C.

refractive index is less than 1.51, and the composition corresponds to a rhyolitic glass.

Infrared absorption studies on these tuffs have shown in the OH-stretch region characteristic vibrations at 3,600 and 3,420 cm<sup>-1</sup>, broad and weak for the rhyolite and ignimbrite and strong for the zeolitic tuff. In contrast, the H-O-H bending frequency of the H<sub>2</sub>O molecule at 1,625 cm<sup>-1</sup> does not occur in the former, but is well defined in the zeolitic tuff. This supports the well-known idea that diagenesis started with hydrolysis of the rhyolitic glass by way of bonding OH to Si groups from the glass, without retaining molecular H<sub>2</sub>O in the vitric material (Hay, 1966, 1977; Surdam, 1977; Lander and Hay, 1993).

The diagenetic facies recognized in the Chichíndaro Formation is the vitric tuff in which glass is altered to smectite + opal-C, indicating diagenesis in a lacustrine environment and

defining the sequence rhyolitic glass → smectite + opal-C. Some associated K-feldspar could devitrify from glass. Close to the contact with the zeolitic tuff, the coexistence of clinoptilolite and smectite is attributed to microenvironmental changes or to incomplete dissolution plus reprecipitation,

Table 7. Chemical composition of unaltered glass and diagenetic minerals of the Chichíndaro Formation.

	Glass	Clinoptilolite	Mordenite	Opal-C
Chemical composition (wt %)				
SiO <sub>2</sub>	77.42	76.70	78.57	97.35
Al <sub>2</sub> O <sub>3</sub>	13.10	14.45	13.67	1.21
TiO <sub>2</sub>	0.08	0.07	0.07	0.04
Fe <sub>2</sub> O <sub>3</sub>	3.26	0.96	0.87	0.28
MnO	0.05	0.06	0.07	0.04
MgO	0.81	0.86	1.52	0.17
CaO	1.65	1.79	2.71	0.23
K <sub>2</sub> O	3.08	4.41	1.76	0.20
Na <sub>2</sub> O	0.55	0.69	0.76	0.48
Total	100.00	99.99	100.00	100.00
Unit-cell contents				
Si		29.56	39.85	
Al		6.55	8.16	
Ti		0.02	0.02	
Fe		0.28	0.33	
Mg		0.49	1.15	
Ca		0.74	1.47	
K		2.17	1.14	
Na		0.51	0.75	
O		72	98	
Si/Al		4.51	4.88	
Si/(Al+Ti+Fe)		4.31	4.68	

Chemical analysis by energy dispersive X-ray coupled to scanning electron microscopy, represent average values. Analysis in weight percent, dry basis. Fe calculated as Fe<sub>2</sub>O<sub>3</sub>.

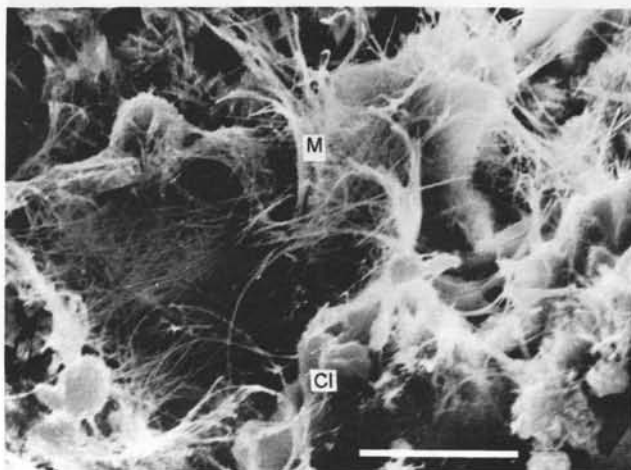


Figure 14. SEM photomicrographs of mordenite. M: mordenite, Cl: clinoptilolite. The fine morphology of mordenite suggests it may have crystallized from solutions. Sample 14, Guanajuato. Horizontal bar represents 10 μm.

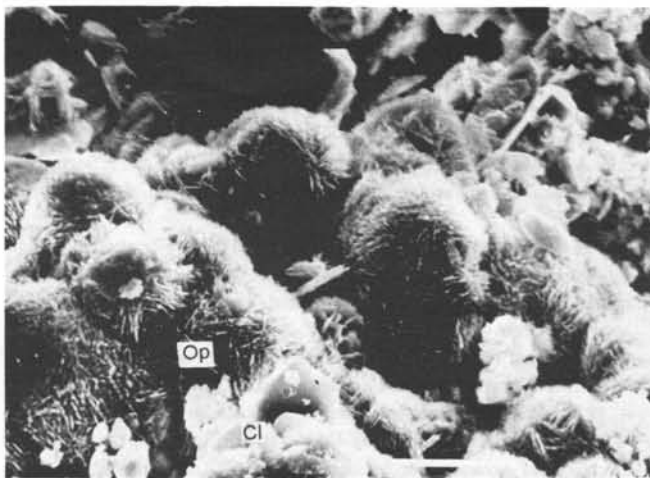


Figure 15. SEM photomicrograph showing crystallization of opal-C and clinoptilolite. Cl: clinoptilolite, Op: opal-C, Guanajuato. Horizontal bar represents 10  $\mu$ m.

rather than to a transformation from one to the other. In the zeolitic tuff, most clinoptilolite resulted from the reactions rhyolitic glass  $\rightarrow$  clinoptilolite + mordenite + opal-C, and rhyolitic glass  $\rightarrow$  clinoptilolite + opal-C, with the probable association of a leaching solution from which the zeolites also crystallized.

The zeolitic tuffs were formed from precursor ash falls of rhyolitic composition. The relations between the various chemical components and  $Al_2O_3$  readily discriminate the ignimbrite of the La Bufa Formation and the overlying rhyolite of the Chichindaro Formation from the vitric and zeolitic tuffs of the Chichindaro Formation. The tuffs have less  $SiO_2$ ,  $K_2O$ , and  $Na_2O$ , more  $MgO$ ,  $CaO$ , and  $H_2O$  and about equal  $Fe_2O_3$  than their rhyolitic precursor. Essentially linear correlations occur between  $Al_2O_3$  and the remaining constituents. Low- $Al_2O_3$  clinoptilolite-containing tuff is associated with relatively high contents of  $SiO_2$ ,  $MgO$ , and  $CaO$  and low  $K_2O$ ,  $Na_2O$ , and  $H_2O$ , whereas high- $Al_2O_3$  clinoptilolite tuff is associated with low  $SiO_2$ ,  $MgO$ , and  $CaO$  and high  $K_2O$ ,  $Na_2O$ , and  $H_2O$ . Correlation among the compositions of rhyolite, vitric tuffs, and zeolitic tuffs of the Chichindaro Formation indicates substantial reductions in the contents of  $SiO_2$ ,  $K_2O$ , and  $Na_2O$  and increases in  $CaO$ ,  $MgO$  from the rhyolite to the zeolitic tuff. The ratios  $SiO_2/Al_2O_3$  and  $SiO_2/Fe_2O_3$  are lower and  $Al_2O_3/Fe_2O_3$  higher in the vitric tuff than in the zeolitic tuff;  $MgO/Al_2O_3$  and  $MgO/Fe_2O_3$  and  $CaO/Al_2O_3$  and  $CaO/Fe_2O_3$  are approximately equal in both tuffs, higher than in rhyolite.  $K_2O/Al_2O_3$  and  $K_2O/Fe_2O_3$  and  $Na_2O/Al_2O_3$  and  $Na_2O/Fe_2O_3$  are about the same in the tuffs and about half of what they are in the rhyolite. The zeolitic tuff contains opal-C from 5% in the most zeolitized material to 20% in the least one. This opal-C appears to accommodate 0.20%  $K_2O$  and 0.48%  $Na_2O$  in its composition; the low content of opal-C in the zeolitic tuff suggests that some silicic acid may have been flushed from the system. This, associated with the absence of smectite in

the zeolite tuff, suggests that diagenesis was in an open hydrologic system.

## GENESIS OF SEDIMENTARY ZEOLITES

### ASSEMBLAGES OF CRYSTALLIZATION

In the sedimentary zeolite deposits of the Sierra Madre del Sur and Sierra Madre Occidental, pyroclastic debris deposited in lacustrine and marine environments shows the following zeolite assemblages: (1) K-feldspar + opal-C; (2) smectite + opal-C; (3) smectite + clinoptilolite + opal-C; (4) clinoptilolite + opal-C; (5) mordenite + opal-C + K-feldspar. Zeolite assemblages have been described for other sedimentary deposits (Surdam, 1977; Hay and Sheppard, 1977; Altaner and Grim, 1990; Sheppard, 1991). The assemblage K-feldspar + opal-C is not universally present and may have been due to crystallization from the precursor rhyolitic glass. The diagenetic alteration to smectite + opal-C is not necessarily associated with zeolites and typifies diagenesis in closed lacustrine environments. Clinoptilolite and mordenite appear to be the two most common zeolites in some regions of Mexico.

### GEOCHEMISTRY OF ZEOLITE DIAGENESIS

Zeolitic tuffs that crop out in the deposits in the Sierra Madre del Sur and in the Sierra Madre Occidental have lower mean contents of  $SiO_2$ ,  $K_2O$ , and  $Na_2O$ , higher  $Al_2O_3$ ,  $MgO$ ,  $CaO$ , and  $H_2O$ , and about the same  $Fe_2O_3$  than the parent rhyolitic precursor ash falls.  $Fe_2O_3$  is essentially constant and  $Al_2O_3$  increases within closed limits with decreasing  $SiO_2$ . In the deposits of the Sierra Madre Occidental, the  $SiO_2/Al_2O_3$  ratios are in the range 4.91 to 7.14, lower in the zeolitic tuff than in the rhyolite or unaltered precursor vitric tuff. Within the zeolitic beds,  $MgO$ ,  $CaO$ ,  $Na_2O$ , and  $K_2O$  remain essentially constant, but the ratios  $(K_2O+Na_2O)/(MgO+CaO)$  change between 2.19 to 0.79, which appear to be necessary to crystallize clinoptilolite. Higher concentrations of alkalis or lower concentrations of alkaline earths that move the ratio outside these ranges do not allow crystallization of zeolite in the studied systems. The correlations confirm the inverse behavior of  $Na_2O$  and  $K_2O$  relative to  $MgO$  and  $CaO$ , release of  $SiO_2$ , and association of clinoptilolite and mordenite with relatively high activities of Ca and Na.

### ACKNOWLEDGMENTS

The authors are indebted to the Programa de Apoyo a Proyectos de Investigación e Innovación Tecnológica of the Universidad Nacional Autónoma de México for its financial support to Project IN106994. Appreciation is manifested to A. Altamira, A. Lozano, A. Maturano, and M. Reyes for their assistance with the analytical work.

## BIBLIOGRAPHICAL REFERENCES

- Alberti, Alberto, 1975, The crystal structure of two clinoptilolites: *Tschermak's Mineralogische und Petrographische Mitteilungen*, v. 22, p. 25-37.
- Alietti, Andrea, 1972, Polymorphism and crystal-chemistry of heulandites and clinoptilolites: *American Mineralogist*, v. 57, p. 1448-1462.
- Altaner, S.P., and Grim, R.E., 1990, Mineralogy, chemistry, and diagenesis of tuffs in the Sucker Creek Formation (Miocene), eastern Oregon: *Clays and Clay Minerals*, v. 38, p. 561-572.
- Ames, L.L., 1960, The cation sieve properties of clinoptilolite: *American Mineralogist*, v. 45, p. 689-700.
- Boles, J.R., 1972, Composition, optical properties, cell dimensions, and thermal stability of some heulandite group zeolites: *American Mineralogist*, v. 57, p. 1463-1493.
- Breck, D.W., *Zeolite molecular sieves—structure, chemistry, and uses*: New York, Wiley and Sons, 600 p.
- CETENAL (actual INEGI), 1973a, [Hoja] Silao (F14-C52): México, D.F., Secretaría de Programación y Presupuesto, Comisión de Estudios del Territorio Nacional, geologic chart, scale 1:50,000.
- 1973b, [Hoja] San Miguel de Allende (F14-C54): México, D.F., Secretaría de Programación y Presupuesto, Comisión de Estudios del Territorio Nacional, geologic chart, scale 1:50,000.
- 1973c, [Hoja] Guanajuato (F14-C53): México, D.F., Secretaría de Programación y Presupuesto, Comisión de Estudios del Territorio Nacional, carta geológica, escala 1:50,000.
- 1973d, [Hoja] Celaya (F14-C64): México, D.F., Secretaría de Programación y Presupuesto, Comisión de Estudios del Territorio Nacional, carta geológica, escala 1:50,000.
- Consejo de Recursos Minerales, 1992, *Monografía geológico-minera del Estado de Guanajuato*: Secretaría de Energía, Minas e Industria Paraestatal, Subsecretaría de Minas e Industria Básica, Monografía, 136 p., 3 maps.
- Cserna, Zoltan de, 1965, Reconocimiento geológico de la Sierra Madre del Sur de México, entre Chilpancingo y Acapulco, Estado de Guerrero: Universidad Nacional Autónoma de México, Instituto de Geología, Boletín 62, 77 p.
- 1975, On the geology of parts of the Trans-Mexico Volcanic Belt and of the Mexican Central Plateau, *in* Pablo-Galán, Liberto de, ed., *International Clay Conference, Field Trip*: Universidad Nacional Autónoma de México, Instituto de Geología, México, D.F., Guidebook FT-1, p. 1-72.
- Hay, R.L., 1966, Zeolites and zeolitic reactions in sedimentary rocks: *Geological Society of America, Special Paper*, v. 85, 130 p.
- 1977, Geology of zeolites: *Mineralogical Society of America, Short course notes*, v. 4, p. 53-64.
- Hay, R.L., and Shepard, R.A., 1977, Zeolites in open hydrologic systems, *in* Mumpton, F.A., ed., *Mineralogy and geology of natural zeolites*: *Mineralogical Society of America, Short course notes*, v. 4, p. 93-102.
- Lander, R.H., and Hay, R.L., 1993, Hydrogeologic control on zeolitic diagenesis of the White River sequence: *Geological Society of America Bulletin*, v. 105, p. 361-376.
- López-Ramos, Ernesto, 1974, *Carta Geológica del Estado de Oaxaca*: Universidad Nacional Autónoma de México, Instituto de Geología, cartas geológicas estatales, scale 1:500,000 (blueprint).
- *Geología de México*: México, D.F., private edition, t. 2, 453 p.
- McDowell, W.F., and Keizer, P.R., 1977, Timing of mid-Tertiary volcanism in the Sierra Madre Occidental between Durango city and Mazatlán, Mexico: *Geological Society of America Bulletin*, v. 88, p. 1479-1487.
- Meier, W.M., 1961, The crystal structure of mordenite (ptilolite): *Zeitschrift für Kristallographie Kristallgeom.*, v. 115, p. 438-450.
- Merkle, A.B., and Slaughter, Maynard, 1968, Determination and refinement of the structure of heulandite: *American Mineralogist*, v. 53, p. 1120-1138.
- Minato, H.; Namba, H.; and Ito, N., 1985, Thermal behaviour of clinoptilolite: *Journal of Mineralogical Society of Japan*, v. 16, pt. 1, p. 101-112.
- Mumpton, F.A., 1960, Clinoptilolite redefined: *American Mineralogist*, v. 45, p. 351-369.
- 1973, First reported occurrence of zeolites in sedimentary rocks of Mexico: *American Mineralogist*, v. 58, p. 287-290.
- 1975, Zeolitic tuffs in the vicinity of Oaxaca, *in* Pablo-Galán, Liberto de, ed., *International Clay Conference, Field Trip*: Universidad Nacional Autónoma de México, Instituto de Geología, México, D.F., Guidebook FT-4, p. 45-57.
- Nieto-Samaniego, Á.F., 1990 (1992), Fallamiento y estratigrafía cenozoicos en la parte sudoriental de la Sierra de Guanajuato: Universidad Nacional Autónoma de México, Instituto de Geología, Revista, v. 9, p. 146-155.
- Ortega-Gutiérrez, Fernando, 1975, Highway geology Mexico-Oaxaca, *in* Pablo-Galán, Liberto de, ed., *International Clay Conference, Field Trip*: Universidad Nacional Autónoma de México, Instituto de Geología, México, D.F., Guidebook FT-4, p. 1-26.
- Ortega-Gutiérrez, Fernando; Mitre-Salazar, L.M.; Roldán-Quintana, Jaime; Aranda-Gómez, J.J.; Morán-Zenteno, Dante; Alaniz-Álvarez, S.A., and Nieto-Samaniego, Á. F., *Texto explicativo de la quinta edición de la carta geológica de la República Mexicana escala 1: 2'000, 000*: Universidad Nacional Autónoma de México, Instituto de Geología, y Secretaría de Energía, Minas e Industria Paraestatal, Consejo de Recursos Minerales, geologic chart, scale 1: 2'000, 000, explanatory text, 74 p.
- Pablo-Galán, Liberto de, 1986, Geochemical trends in the alteration of Miocene vitric tuffs to economic zeolite deposits, Oaxaca, Mexico: *Applied Geochemistry*, v. 1, p. 273-285.
- Pablo-Galán, Liberto de; Chávez-García, M.L.; and Dimas, Guadalupe, 1994, Diagenesis of Miocene vitric tuffs to zeolites, Mexican highlands, Mexico: *Mineralogical Magazine*, v. 58A, p. 682-683.
- Pablo-Galán, Liberto de, and Chávez-García, M.L., 1996, Diagenesis of Miocene vitric tuffs to zeolites, Mexican Volcanic Belt: *Clays and Clay Minerals*, v. 44, p. 324-338.
- Sheppard, R.A., 1991, Zeolitic diagenesis of tuffs in the Miocene Chalk Hills Formation, western Snake River Plain, Idaho: *U.S. Geological Survey Bulletin*, v. 1963, p. 1-27.
- Surdam, R.C., 1977, Zeolites in closed hydrologic systems, *in* Mumpton, F.A., ed., *Mineralogy and geology of natural zeolites*: *Mineralogical Society of America, Short course notes*, v. 4, p. 65-91.
- Wilson, J.A., and Clabaugh, S.E., 1970, New Miocene formation, and a description of volcanic rocks, northern valley of Oaxaca, State of Oaxaca, *in* Segura, L.R., and Rodríguez, Rafael, eds., *Libro Guía de la Excursión México-Oaxaca*: México, D.F., Sociedad Geológica Mexicana, Libro-guía, p. 120-128.

Manuscript received: March 7, 1996.

Corrected manuscript received: June 29, 1996.

Manuscript accepted: July 5, 1996.